

D. DOLMATOV, MASOUD HAJIVAND

ON LOW-EMISSION ANNULAR COMBUSTOR BASED ON DESIGNING OF LINER AIR ADMISSION HOLES

Numerical experiments was carried out to predict the total temperature characteristics and formation of nitrogen oxide emissions and pattern factor in an annular combustor liner based on geometrical parameters and location and rows of different air admission holes, for 6 various cases, using computational fluid dynamics (CFD). The simulation has been performed using ANSYS CFX including finite rate chemistry and eddy dissipation model, for simulation of liquid kerosene (Jet A) – air combustion after fuel droplet evaporation. The spray modeling was performed, including Rosin-Rammler droplet distribution. Thermal and prompt nitrogen oxide (NO_x) formation was performed to predicting NO_x emission characteristics with a $k-\epsilon$ model of turbulent. In this investigation the 3D CAD model of the realistic annular combustion chamber is presented for the simulation with double radial air swirler for the better mixing fuel with air. Beside this the characteristic and the flame structure is presented including the contour plots of total temperature and NO concentration at the outlet of the combustor liner and in cross section plane along the X axis from the injector center of the combustor including the chart of the velocity and NO, CO, CO_2 , O_2 and the total temperature along the liner from the injector center. For the combustion of kerosene with air 2 step kinetic schemes are presented in this study. The results show that the best result with the low concentration of NO is the case 5 but with a high percentage of pressure drop and the case 3 have the maximum concentration of NO with the low percentage of pressure drop.

Keywords: Rosin-Rammler – emission-nitrogen oxide-CFD-annular combustor-pattern factor

Д. А. ДОЛМАТОВ, МАСУД ХАДЖИВАНД

НИЗКОЕМИСИЙНА КІЛЬЦЕВА КАМЕРА ЗГОРЯННЯ, СПРОЕКТОВАНА З РІЗНИМИ ВАРИАНТАМИ ОТВОРІВ ДЛЯ ПОДАЧІ ПОВІТРЯ

Проведено чисельні експерименти для прогнозування температурних характеристик, утворення викидів оксидів азоту (NO_x) і коефіцієнта рівномірності поля температури на виході з кільцевої камери згоряння на основі геометричних параметрів, місця розташування і кількості рядів отворів для подачі повітря в шість різних випадках з використанням обчислювальної гідродинаміки (CFD). З використанням ANSYS CFX, включаючи хімію кінцевих швидкостей і модель вихрової дисипації, виконано чисельне дослідження згоряння рідкого гасу (Jet A) після випаровування крапель палива. Проведено моделювання розпилення, включаючи розподіл крапель Розіна-Раммлера. Для прогнозування емісійних характеристик з використанням $k-\epsilon$ моделі турбулентності виконано моделювання утворення термічних і швидких оксидів азоту.

Ключові слова: розподіл крапель Розіна-Раммлера, утворення викидів оксидів азоту, обчислювальна гідродинаміка, кільцева камера згоряння, коефіцієнт рівномірності поля температури.

Д. А. ДОЛМАТОВ, МАСУД ХАДЖИВАНД

НИЗКОЭМИССИОННАЯ КОЛЬЦЕВАЯ КАМЕРА СГОРАНИЯ, СПРОЕКТИРОВАННАЯ С РАЗЛИЧНЫМИ ВАРИАНТАМИ ОТВЕРСТИЙ ДЛЯ ПОДАЧИ ВОЗДУХА

Проведены численные эксперименты для прогнозирования температурных характеристик, образования выбросов оксидов азота (NO_x) и коэффициента равномерности поля температуры на выходе из кольцевой камеры сгорания на основе геометрических параметров, местоположения и количества рядов отверстий для подачи воздуха в шесть различных случаях с использованием вычислительной гидродинамики (CFD). С использованием ANSYS CFX, включая химию конечных скоростей и модель вихревой диссипации, выполнено численное исследование сгорания жидкого керосина (Jet A) после испарения капель топлива. Проведено моделирование распыления, включая распределение капель Розина-Раммлера. Для прогнозирования эмиссионных характеристик с использованием $k-\epsilon$ модели турбулентности выполнено моделирование образования термических и быстрых оксидов азота.

Ключевые слова: распределение капель Розина-Раммлера, образование выбросов оксидов азота, вычислительная гидродинамика, кольцевая камера сгорания, коэффициент равномерности поля температуры.

Introduction

The design of a gas turbine combustor is a difficult and multidisciplinary task which is based on a large variety of design rules and empirical correlations. Some of the main design targets are the achievement of low emission levels, low pressure losses and a satisfactory level of uniformity of the thermodynamic properties distribution in the gas outflow including thermo-acoustic waves and noise and, stability and structural integrity with a very stable combustion process under a wide range of working conditions. Numerical and experimental analysis must be carried out to verify if the targets have been fulfilled and to refine the combustor design by means of

an expensive and time consuming iterative procedure [1]. Beside that we need to remember that numerical simulations should be carried out with special care, means with the deep knowledge of assumptions made in the mathematical model and of physical aspects of investigated phenomena.

Most of the design requirements of a combustor are contradicting and conflicting in nature such as the circumferential Pattern factor (CPF) which indicates the quality of the combustor exit temperature distribution and dictates the turbine vane life can be reduced by having a larger pressure drop across the combustor liner resulting in an enhanced mixing and turbulence inside the liner, whereas, the total pressure loss in a gas turbine combustor has to be a minimum as every-

© D. A. Dolmatov, Masoud Hajivand, 2018

one percentage increase in pressure loss can result in either a half percent reduction in thrust or around a quarter of a percent increase in specific fuel consumption [2].

Ground level ozone is formed in a complex reaction between NO_x and reactive organic compounds. There are many natural sources of reactive organics but most NO_x is produced mainly from combustion of hydrocarbon fuels such as natural gas, oil, and coal. Natural gas is the cleanest burning hydrocarbon fuel, but all flames owing to their high temperature have the potential to produce NO_x . Most commonly nitric oxide (NO), a fusion of the naturally occurring nitrogen and oxygen in air exposed to high temperature [3].

Combustion control may involve any of 3 strategies such as reducing peak temperatures in the combustion zone, reducing the gas residence time in the high-temperature zone and reducing oxygen concentrations in the combustion zone [4]. These changes in the combustion process can be achieved either through process modifications or by modifying operating conditions and geometrical parameters such as designing air admission and cooling holes on combustion chamber liners which are presented in this study. In other words several technologies have been presented in recent decades for reducing NO_x emissions in aircraft gas turbines. The most well-known are the Water-Steam Injection, Rich burn Quick Quench-Lean Burn (RQL), Lean Premix Pre-vaporized (LPP), and the Lean-Direct Injection (LDI) engine.

The internal flow of an aircraft engine combustor consists of complicated phenomena, including turbulent mixing along with spraying, atomizing, and swirling of liquid fuel, as well as a huge number of chemical reaction mechanisms, reproduction through numerical simulation is very difficult, and even today there are few tools with sufficiently high prediction accuracy for this purpose. In recent years, Large Eddy Simulation (LES), which has a small number of adjustment parameters for modeling and can simulate unsteady turbulent flow, has attracted a great deal of attention. However, LES has not been established as a practical design tool for actual combustors, because the atomization model and turbulence combustion model for the spray combustion field of LES are still in the study phase and the calculation load of LES is very high, therefore, significant computer resources are required [5].

Accordingly, the main method used in current practice is Reynolds-Averaged Navier-Stokes (RANS) simulation, which obtains a steady mean field where turbulence phenomena are averaged. RANS simulation has lower accuracy than LES, but it can be used sufficiently as a design tool through proper interpretation of its results due to its reasonable computational costs [6].

Several researchers have used CFD effectively to analyze and optimize gas turbine combustors such as Koutsenko I. G. et. al. [7] have optimized a gas tur-

bine combustor to achieve a low level of nitric oxide emissions through CFD analyses. The commercial CFD code 'CFX-TASC Flow' was used for calculating the flow structure and for analyzing the nitric oxide formation process inside the combustor. By suitably modifying the distribution of secondary air through alterations to the arrangement of primary and dilution zone holes, the combustor was optimized.

Rudolph D. et al. [8], developed the Advanced Combustion Tool (ACT) CFD process to rapidly analyze the performance of a gas turbine combustor from a given fuel injector, CAD geometry and engine cycle information.

Constantinescu, G. et. al., [9] have developed and presented the main features of a three dimensional Large Eddy Simulation (LES) two-phase flow code using unstructured meshes to simulate non-reacting and reacting flows through realistic combustors. The use of this code was tested and demonstrated on realistic combustor geometry (Pratt & Whitney Combustor). Results from these simulations showed the superior predictive capabilities of LES techniques compared to RANS based flow solvers for predicting flow, turbulent mixing and combustion phenomena in combustors. Jiang Leiyong and Campbell Ian [10] have made an attempt to analyze flow in a gas turbine combustor using LES considering a few important issues like grid size, inflow condition, wall boundary conditions, physical sub-models and data sampling. James S. et. al. [11] presented an assessment of Large Eddy Simulation (LES) and conventional Reynolds-Averaged Navier-Stokes methods (RANS) for predicting aero-engine gas turbine combustor performance, which as per the authors is the first systematic assessment of LES versus RANS on industry-relevant aero-engine gas turbine combustors.

Purpose of this study

The purpose of this study is to predict the total temperature characteristics and formation of harmful pollutant such as nitrogen oxide emissions (NO), CO and CO_2 and pattern factor in an annular combustor liner exit based on geometrical parameters and location and rows of different air admission holes (primary, secondary and dilution holes), for 6 various cases, using computational fluid dynamics (CFD). The simulation has been performed using ANSYS CFX including finite rate chemistry and eddy dissipation model, for simulation of liquid kerosene (Jet A) – air combustion after fuel droplet evaporation. The spray modeling was performed, including Rosin-Rammler droplet distribution. Thermal and prompt nitrogen oxide (NO_x) formation was performed to predicting NO_x emission characteristics with a $k-\epsilon$ model of turbulent. The simulation was performed on a 3D CAD model of realistic aero-engine annular combustor. The contour plots of total temperature and NO distribution at the

exit and the axial plane of the liner are shown including velocity distribution along the liner.

Governing equations and turbulence model

The mathematical equations describing the fuel combustion are based on the equations of conservation of mass, momentum, and energy together with other supplementary equations for the turbulence and combustion. In this investigation the standard k - ε turbulence model is used. The equations for the turbulent kinetic energy k and the dissipation rate of the turbulent kinetic energy ε are solved several models of turbulence have been put forward by different authors. These models differ in complexity and range of applicability; they also involve the solution of different numbers of differential equations. The turbulence model incorporated in this work is the high Reynolds number k - ε two equation model. This model requires the solution of two differential equations, for the two turbulence properties: the kinetic energy of turbulence k , and its dissipation rate ε . The model is moderate in complexity. It has been extensively used by many investigations and has proved to be adequate over a wide range of flow situation. The governing differential equations are presented by (Launder, and Spalding, 1974).

Combined EDM/Finite Rate Chemistry combustion Model

For the combined Finite Rate Chemistry/Eddy Dissipation Model, the reaction rates are first computed for each model separately and then the minimum of the two is used. This procedure is applied for each reaction step separately, so while the rate for one step may be limited by the chemical kinetics, some other step might be limited by turbulent mixing at the same time and physical location. It is also possible to apply different combustion models to each of the steps in a multi-step scheme. Some of the predefined schemes make use of this feature, regardless of the global model selection. The combined model is valid for a wide range of configurations, provided the flow is turbulent. In particular, the model is valid for many reactions that range from low to high Damköhler numbers (chemistry slow/fast compared to turbulent time scale). Use of this model is recommended if reaction rates are limited by turbulent mixing in one area of the domain and limited by kinetics somewhere else. The Eddy Dissipation model can, however, be more robust than Finite Rate Chemistry or the combined model [12].

The Eddy-Dissipation Model

The Eddy Dissipation model is best applied to turbulent flows when the chemical reaction rate is fast relative to the transport processes in the flow. There is

no kinetic control of the reaction process. Thus, ignition and processes where chemical kinetics may limit reaction rate may be poorly predicted [12]. This turbulence-chemistry interaction model is based on the work of [13]. The net rate of production for species i due to reaction r , is given by the smaller of the two expressions below:

$$R_{i,r} = v_{i,r} M_{\omega,i} A \rho \frac{\varepsilon}{k} \min \left(\frac{Y_R}{v_{R,r} M_{\omega,R}} \right), \quad (1)$$

$$R_{i,r} = v_{i,r} M_{\omega,i} A B \rho \frac{\varepsilon}{k} \min \left(\frac{\sum_P Y_P}{\sum_j v_{j,r} M_{\omega,j}} \right). \quad (2)$$

Where Y_R is the mass fraction of a particular reactant R , Y_P is the mass fraction of any product species P and A , B are empirical constants equal to 4, 0.5 respectively.

The Finite Rate Chemistry Model

The Finite Rate Chemistry model, as implemented in CFX, assumes that the rate of progress of elementary reaction k can be reversible only if a backward reaction is defined. [13]. Therefore, the rate of progress $\bar{R}_{i,r}$, is computed as:

$$\bar{R}_{i,r} = (v'_{i,r} - v''_{i,r}) \left[k_{f,r} \prod_{j=1}^N [C_{i,r}]^{\eta'_{j,r}} - k_{b,r} \prod_{j=1}^N [C_{j,r}]^{\eta''_{j,r}} \right], \quad (3)$$

where N – is the number of chemical species in the system;

$v'_{i,r}$ – is the stoichiometric coefficient for reactant i in reaction r ;

$v''_{i,r}$ – is the stoichiometric coefficient for product i in reaction r ;

$k_{f,r}$ – is the forward rate constant for reaction r and $k_{b,r}$ is the backward rate constant for reaction r ;

$C_{i,r}$ – is the molar concentration of species j in reaction r ;

$\eta'_{j,r}$ – is the rate exponent for reactant species j in reaction r ;

$\eta''_{j,r}$ – is the rate exponent for product species j in reaction r .

The only built-in formula for the forward and backward rate constants assumes an Arrhenius temperature dependence as:

$$F_k = B_k = A_k T^{\beta_k} \exp \left(\frac{E_k}{RT} \right), \quad (4)$$

where A_k – is pre-exponential factor;

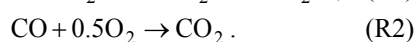
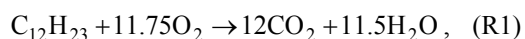
β_k – is the temperature exponent (dimensionless);

E_k – is the activation energy;

T – is the absolute temperature [13].

Combustion reaction and NO mechanism

The combustion reaction of Jet A with air is modeled by a single species surrogate. A two-step global mechanism for Jet A ($C_{12}H_{23}$) is employed, which consists in a first step for fuel oxidation into CO and H_2O , and a second step for CO oxidation into CO_2 :



Arrhenius coefficients for this scheme can be found in [14].

Predominant source of NO_x in gas flames at temperatures above 1800 K. N and O radicals abundant at high temperatures. Dominated by two reactions Zeldovich mechanism (1947).



Two NO molecules formed if reaction 3 is combined with either of reactions 4 or overall reaction:



3D model of annular combustor, meshing and boundary condition

Aero-engine annular combustor assembly consists of many different elements and parts and small design details, such as injecting devices, mounting brackets and flanges or buckets on the holes.

This simulation was performed on a 20 degree sector of a realistic aero-engine annular combustor. The CAD 3D model of the combustor with the double radial swirler and the fuel injector are shown in fig. 1 including air admission holes on the liner. Liquid Kerosene ($C_{10}H_{23}$, Jet A) and air are entered in the domain separately.

The sector of annular combustor was meshed for simulating in an unstructured tetrahedrons meshing method, with about total number of 7.905.624 elements for the combustor with minimum number of holes on the liner, and 8.288.828 for the combustor with maximum number of holes. Including prismatic layers around the walls of annular combustor. The meshes are shown in 2D cross section plane fig. 2.

The air entering combustor inlet have a temperature of 860 K with the mass flow rate of 1.8 kg/s and average static pressure of 28 atm at the outlet. The fuel temperature was 430 K injected from the injector surface with the velocity of 18 m/s and the mass flow of 0.03 kg/s. Atomization of liquid fuel with particle droplet distribution obey Rosin-Rammler law with average drop diameter $d = 30$ micron and non-uniform exponent $n = 2.5$. The radius of injection plane is 3mm with hollow cone angle of 40 degree.



Fig. 1 – 3D CAD model of combustor

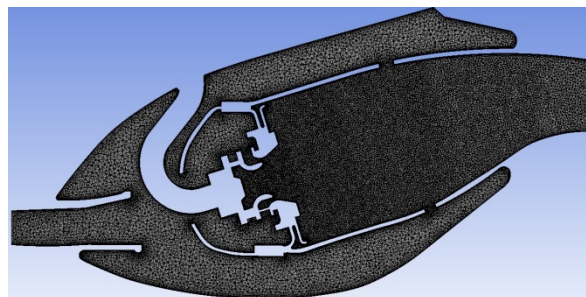


Fig. 2 – 2D view of the cross-section meshes

Cases of this study

In this numerical experiment 6 cases of annular combustor, with different geometrical parameters, numbers, location and rows of air admission holes on the outer and inner liner, were studied. The form of holes are circular on the liner. The angle of holes are 90 degrees on the liner relative to the injector axis shown in Fig. 3, except for case 5 which is 45 degrees for the second row of holes.

The strategy of location of the holes on the outer and the inner liner are shown in Fig. 3. The location of inner liner holes obey the outer which is clear from the Fig. 3, they are parallel and had the degree of 90 relative to the injector axis. The line 1 show the location of the first row of holes for inner and outer liner and line 2 show for the hole location for the second row of holes. The first 4 cases are shown in Fig. 4.

The location and the geometrical parameters of the air admission holes is clear in the case 1. For the case 2 we moved the first row of the holes closer to the primary zone of the combustion in the liner. According to the case 2, for the case 3 we added the third rows of holes closer to the dilution zone and for the case 4, according to the case 2 we added one row closer to the first row of the holes and another row closer to the third row. The main thing that for the case 5 as we said above the angle of the holes on the liner on the second row is 45 degrees relative to the injector axis and for the case 3 according to the case 1 the geometry of the all holes is 1.25 times bigger than the case 1.

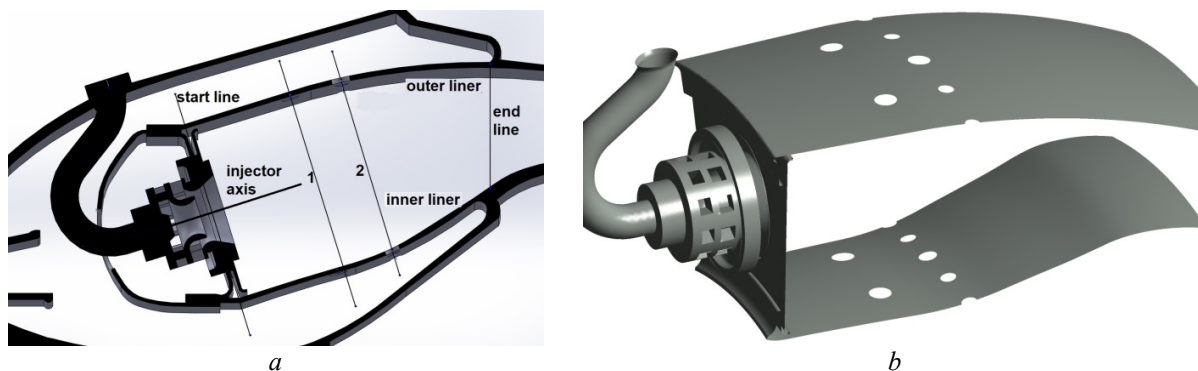


Fig. 3 – The strategy of location: *a* – of the holes on inner and outer of the combustor; *b* – liner with holes

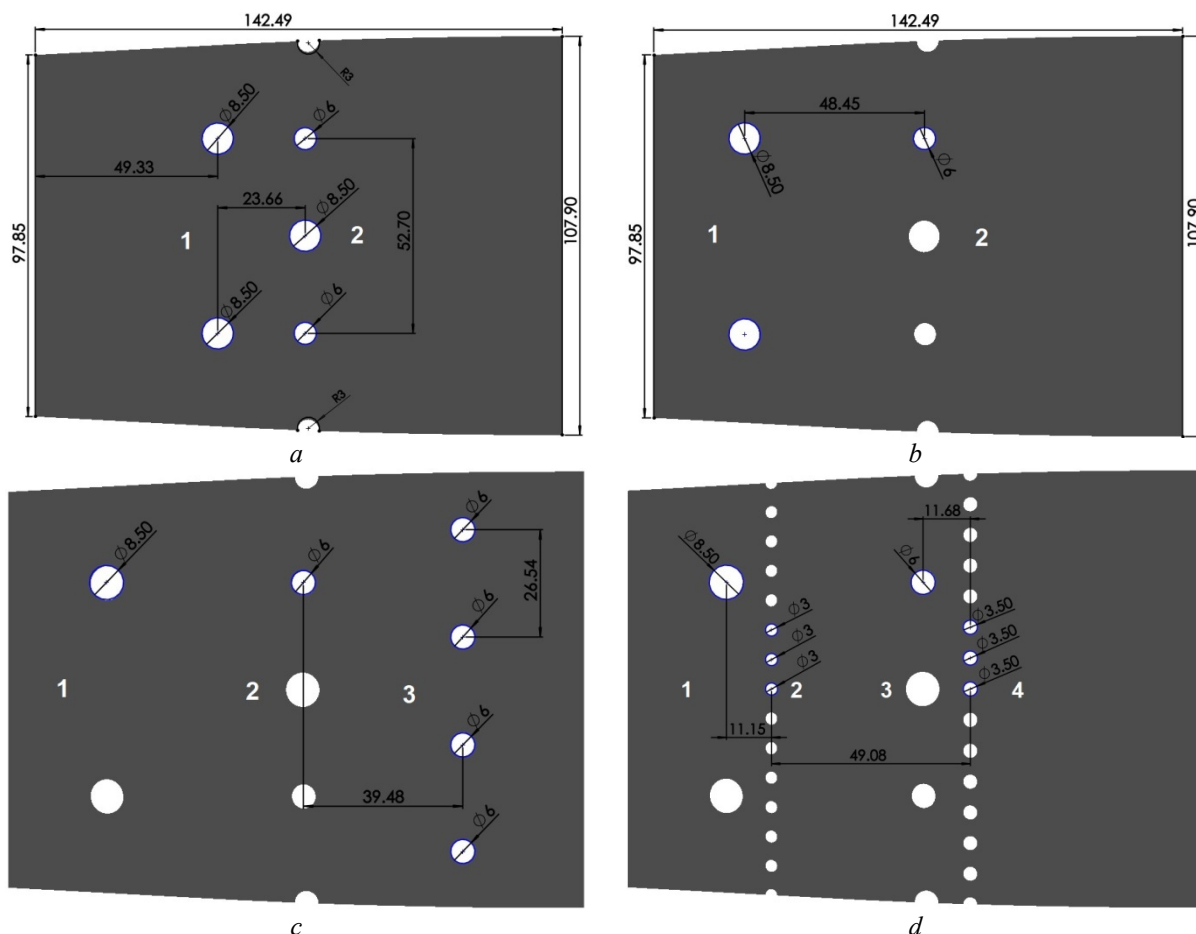


Fig. 4 – The circular geometrical parameters of the liner holes with location and number of the holes and rows for: *a* – case 1; *b* – case 2; *c* – case 3; *d* – case 4

Results and discussion-Temperature distribution

The performed numerical analysis of the flow in the annular combustion chamber of aero engine with the various cases of air admission holes location and its geometrical parameters with different rows, allow to accurately estimating the percentage of air distribution in the different zones of the liner, which was the main objectives of this work. The temperature distribution along the axial cross section of the combustor was shown for 6 various cases in Fig. 5.

According to this simulation analysis results, the

distribution of the temperature along the axial cross section, shows that the airflow passing through the air holes admission into the liner strongly dependent on the location and the number of rows of this holes on the liner. The temperature raises to maximum (2732.315 K) which is for case 4 who has the maximum number of holes with the maximum number of rows, because the first 2 rows is closer to the primary combustion zone who makes the quick mixing better with the entered airflow. Case 4 has the highest total temperature in the primary zone of combustion in this investigation.

Beside that, it was found that the maximum temperature of 2716.460 K, for case 3 is closer to the maximum temperature for case 4. For the case 2 the maximum temperature is 2633.492 K which has a single row of air admission holes closer to the primary zone too. For the case 1, 5, 6 we can see that they hold the minimum total temperature along the axial cross section because there are not air admission holes in the area of combustion primary zone and it can be seen that there are a poor mixing in these areas for not adequate airflow.

For the outlet temperature which is shown in Fig. 6 we can see that, the location and number of rows of air admission holes on the combustor liner strongly effect on the temperature uniformity at the outlet of the liner as shown in Fig. 6.

The highest temperature is for cases 1, 2, 3, 6. In these cases the location and number of rows are different, this means that the temperature increased in case 2 to 1692 K in comparison with case 1, when the first row of holes move closer to the primary zone of combustion and this make the flame, stretching downstream to the outlet with a narrow high temperature of the flame. In case 1 as the same case 2, but the first row is closer to the second zone of combustion but the temperature is lower. In case 3, added one row of holes closer to the dilution zone but the significant effect were not seen at the outlet of the liner but the uniformity of temperature distribution is different. The minimum outlet temperature of 1551 K is for case 4 which have the maximum number of rows on the liner with different sizes. In this case the uniformity of temperature distribution is different from the other cases. There are two rows of holes: first rows is the same as case 2, we added the second row closer to the first row with more number of holes with minimum diameter of 3 mm and the forth row closer to the third row. Here we have the minimum temperature at the out let because of maximum quantity of airflow entering the liner. The geometry and the number of rows of the holes are the same as in case 1, but the angel of the holes on the liner on the second rows is 45 degrees relative to the injector axis. Here the maximum temperature is 1586 K so the air flow enters the liner under a specific angel, to the liner in dilution zone region. And for the case 6 we have the geometry like the first case but the diameter of the holes are 1.25 time larger than the holes in case 1 so we have the temperature of 1665 K. This means with increasing the size of holes diameters the temperature raises at the same time.

NO distribution

The contour map of NO distribution and concentration in ppm, in the meridional mid plane is shown in Fig. 7. For the first case the maximum percentage

of NO is 95.6 ppm around the swirler dome. For case 2 by moving the first row of holes closer to the primary zone of combustion the NO percentage became more, up to 1541.4 ppm because of the quick mixing which happens in the primary zone of combustion. In case 3 the maximum percentage of NO is 9034 ppm in primary zone. In this investigation the case 3 has the maximum NO in the primary zone of the combustion.

Beside that for the case 4 the maximum no is 5886 ppm with the maximum number of holes and the NO formed in the primary region of combustion downstream to the outlet. The maximum NO in case 5 is 26.5 ppm which is the minimum percentage of NO in this investigation. In this case the second rows are under the 45 degree relative to the injector axis, which they are situated closer to the dilution zone. And for the case 6 the maximum percentage of NO is 161.5 ppm when the diameter of holes is bigger then the holes in case 1.

In Fig. 8 it is clear that the minimum percentage of NO at the outlet exit plane of the liner, is for case 1, 5, 6. By observing the various variants of study on designing air admission holes on the liner, we can say that the cases who have the first rows of the holes, far from the primary zone of the combustion, have the lower concentration of NO at the outlet with the second row of holes closer to the dilution zone. by adding holes on case 2, 3, 4 we reached the highest level of NO. Case 2 has the 210 ppm of NO, for the case 3 by adding one row closer to the dilution region we reached 1260 ppm of NO. Beside that there is not a significant difference between the case 3 and 4 for the maximum concentration of NO but it can be seen a significant difference about the uniformity of the outlet NO. It is clear that the minimum concentration of NO is for case 5, about 11 ppm of NO at outlet and 61.5 ppm for the case 6.

The velocity distribution contours at the cross section plane of the combustor

The results show that for each case of study with different location and rows number of air admission holes we reached different velocity magnitude characteristic along the axial cross section of combustor which are shown in Fig 9. The CFD simulation described earlier has been applied to the fully coupled calculations, including both annulus and core-flow. The contour map of velocity magnitude in the meridional mid plane is shown in Fig. 9. As expected there is acceleration through the Venturi of the injection system. The primary zone is created by the sudden expansion of the both swirling flows discharging into the combustor Note also the effects of air penetration through the dilution holes that illustrate extreme complexity of such flows.

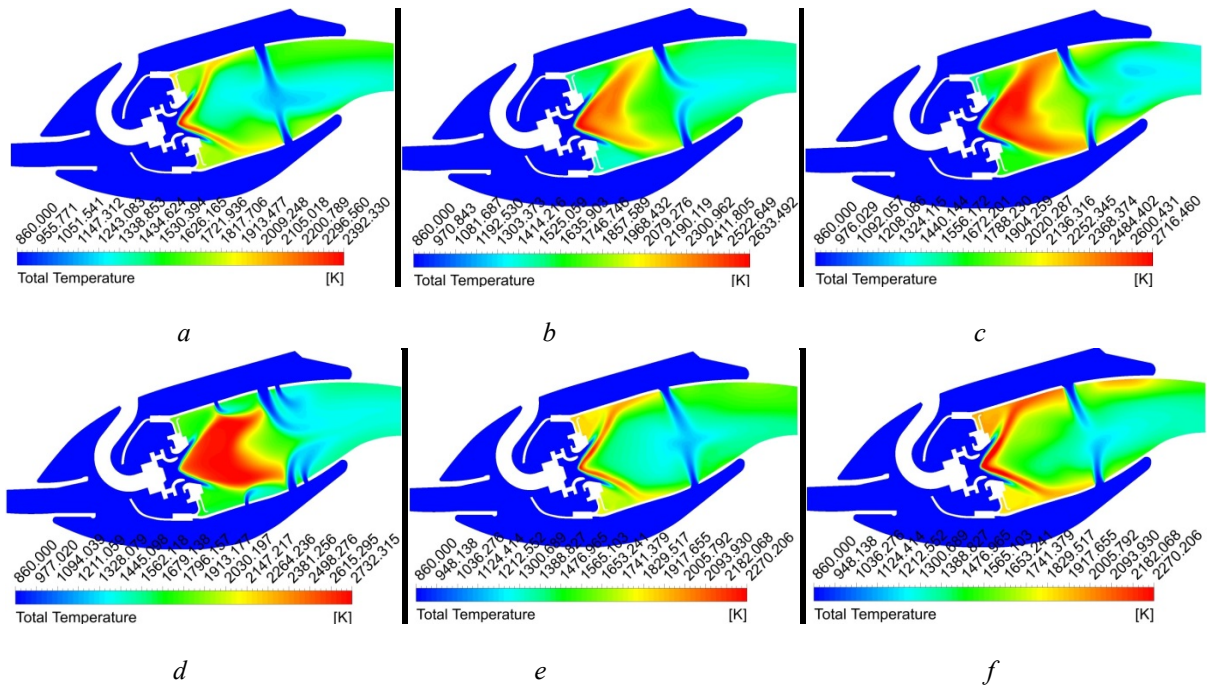


Fig. 5 – The cross section of total temperature distribution contours for:
 a – case 1; b – case 2; c – case 3; d – case 4; e – case 5; f – case 6

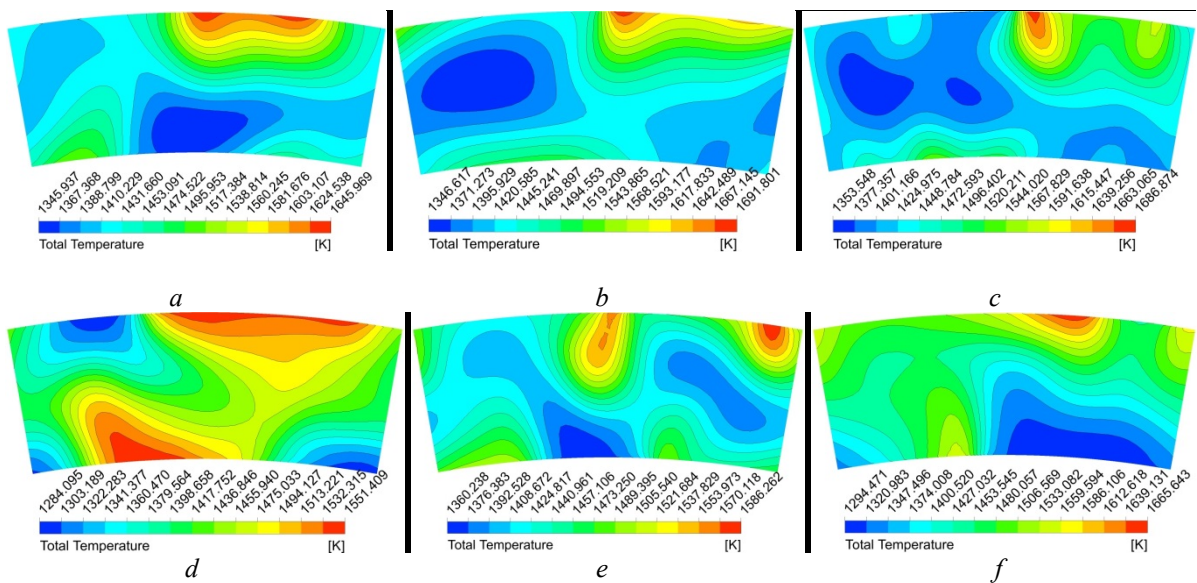
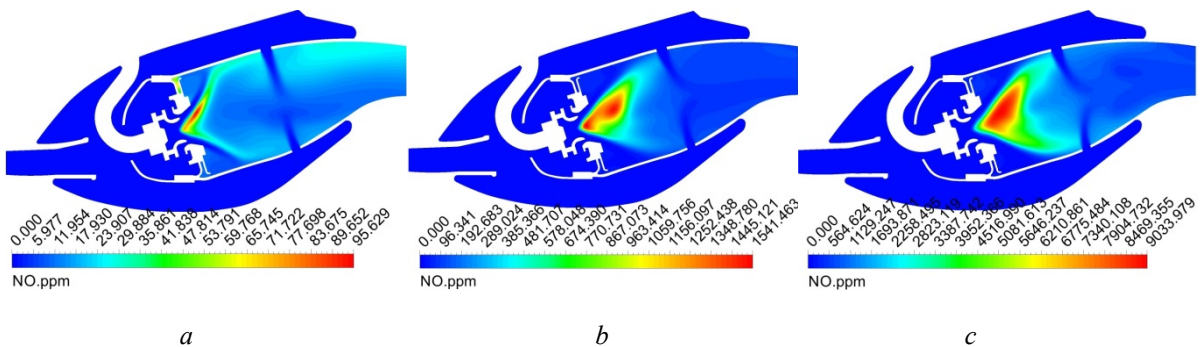


Fig. 6 – The outlet temperature contours for:
 a – case 1; b – case 2; c – case 3; d – case 4; e – case 5; f – case 6



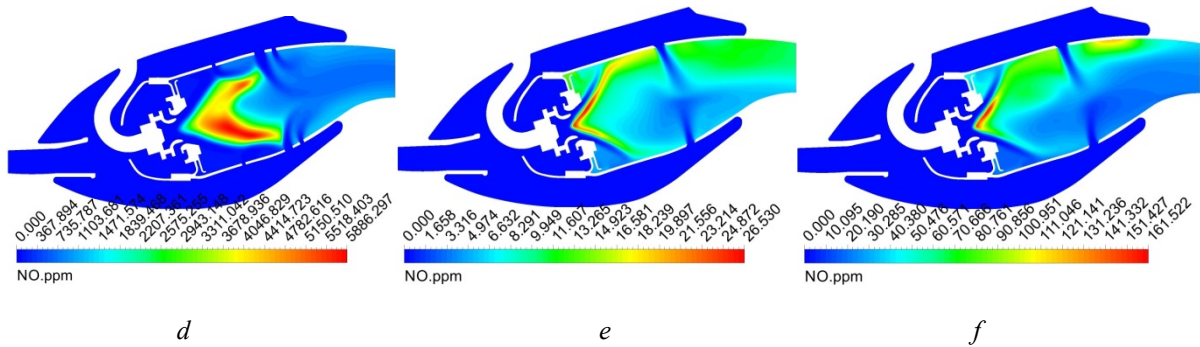


Fig. 7 – The NO distribution contours along the cross section plane for: a – case 1; b – case 2; c – case 3; d– case 4; e – case 5; f– case 6

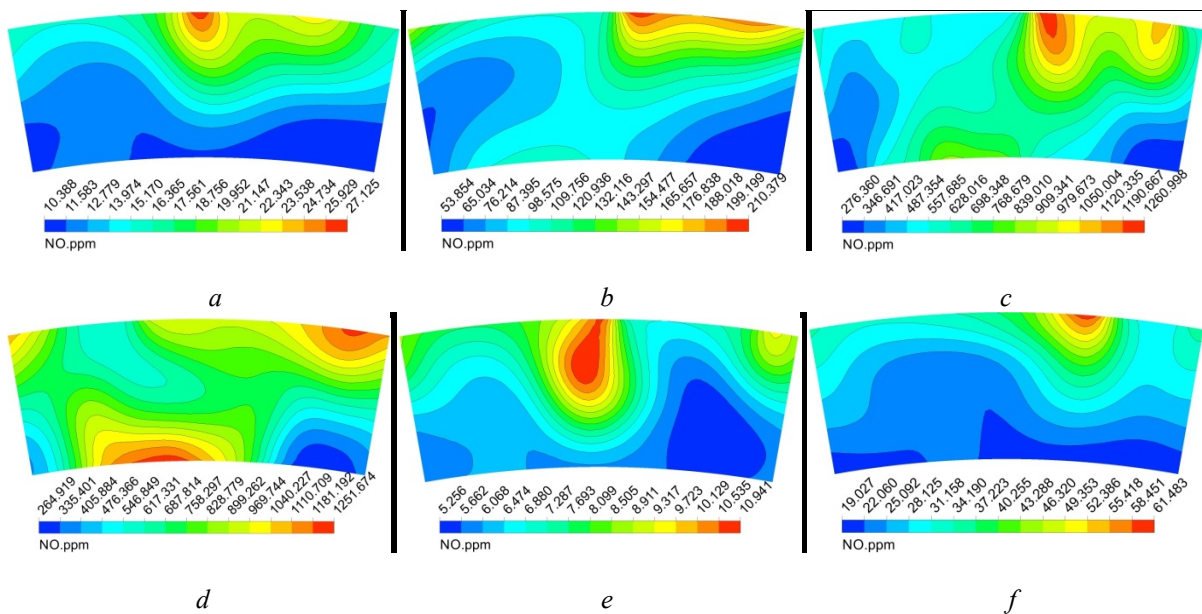


Fig. 8 – The NO distribution contours at the outlet exit plane for: a – case 1; b – case 2; c – case 3; d– case 4; e – case 5; f– case 6

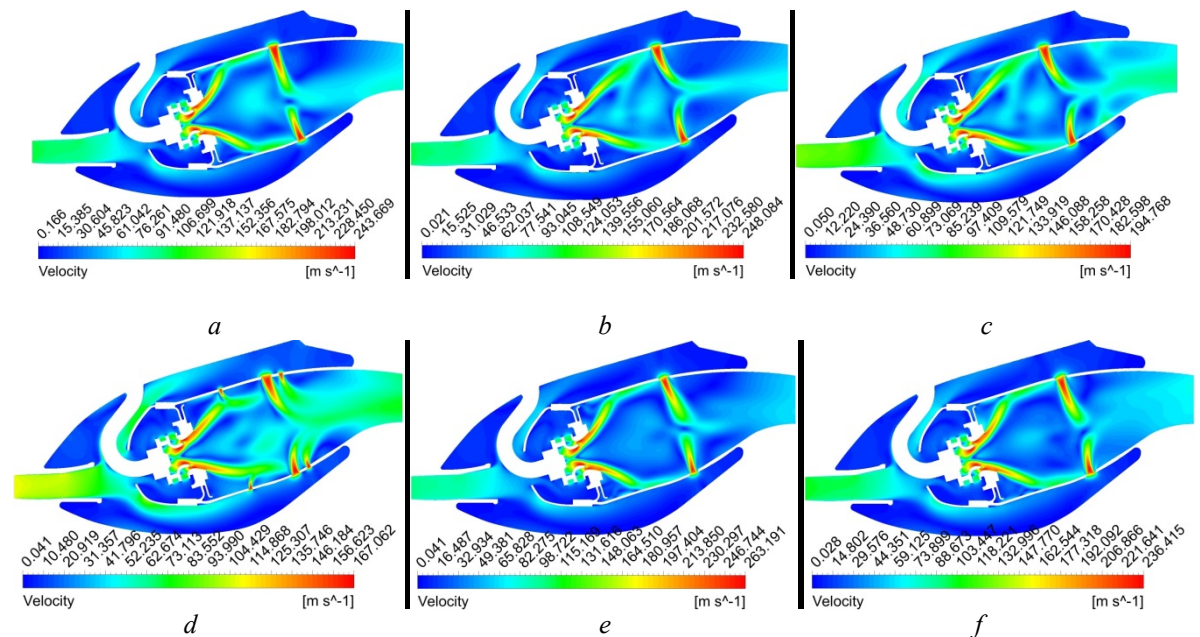


Fig. 9 – velocity distribution contours for: a – case 1; b – case 2; c – case 3; d– case 4; e – case 5; f– case 6

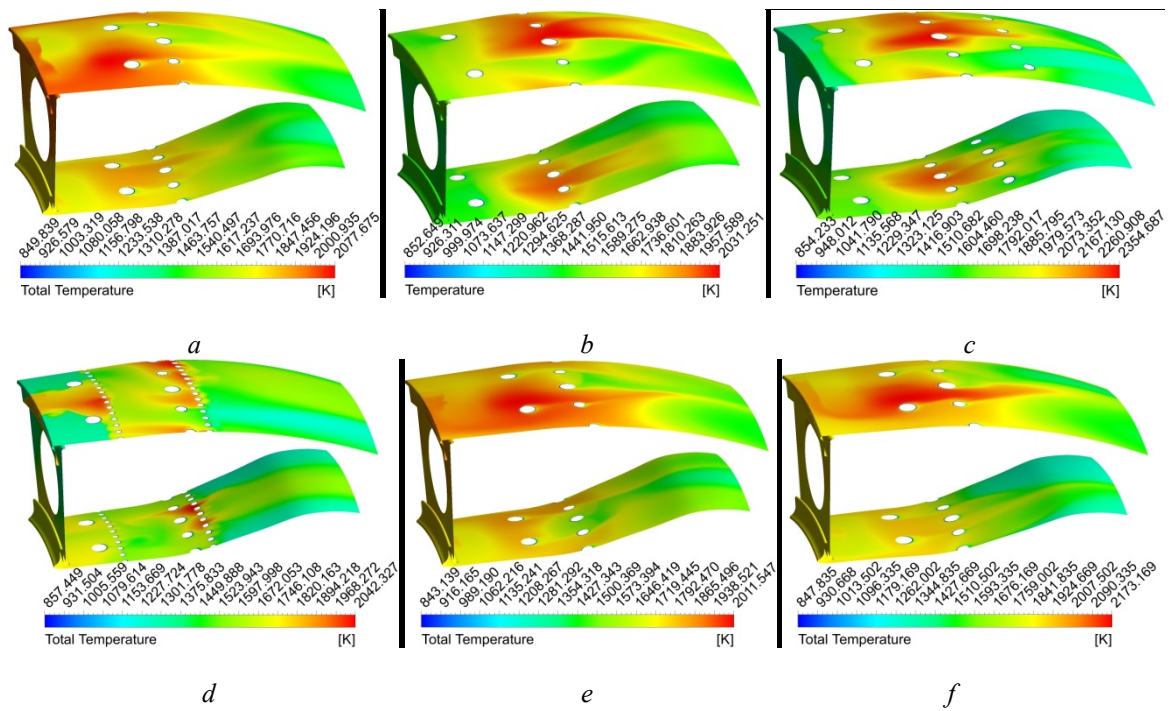
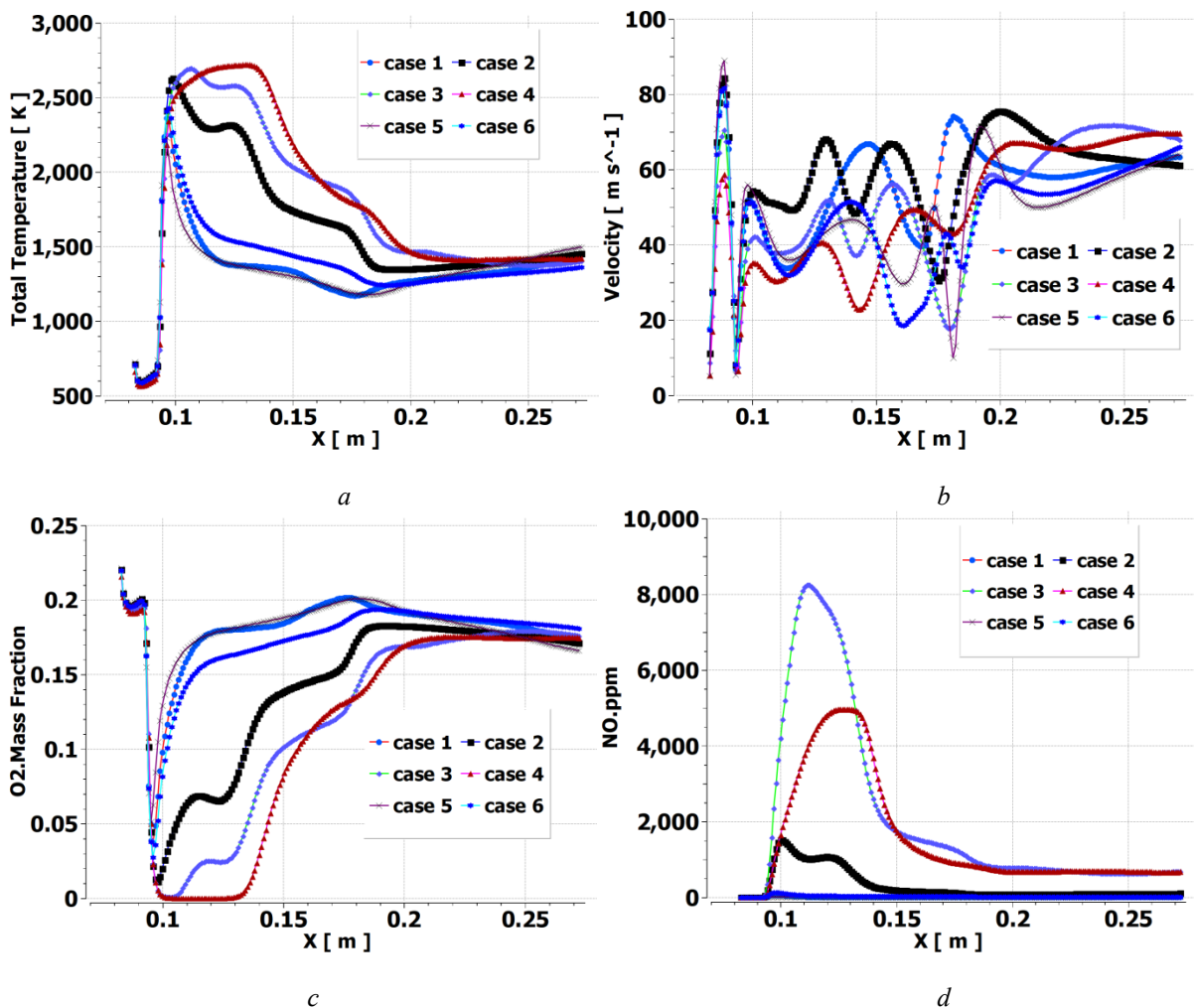


Fig. 10 – Wall temperature distribution for:
a – case 1; *b* – case 2; *c* – case 3; *d*– case 4; *e* – case 5; *f*– case 6



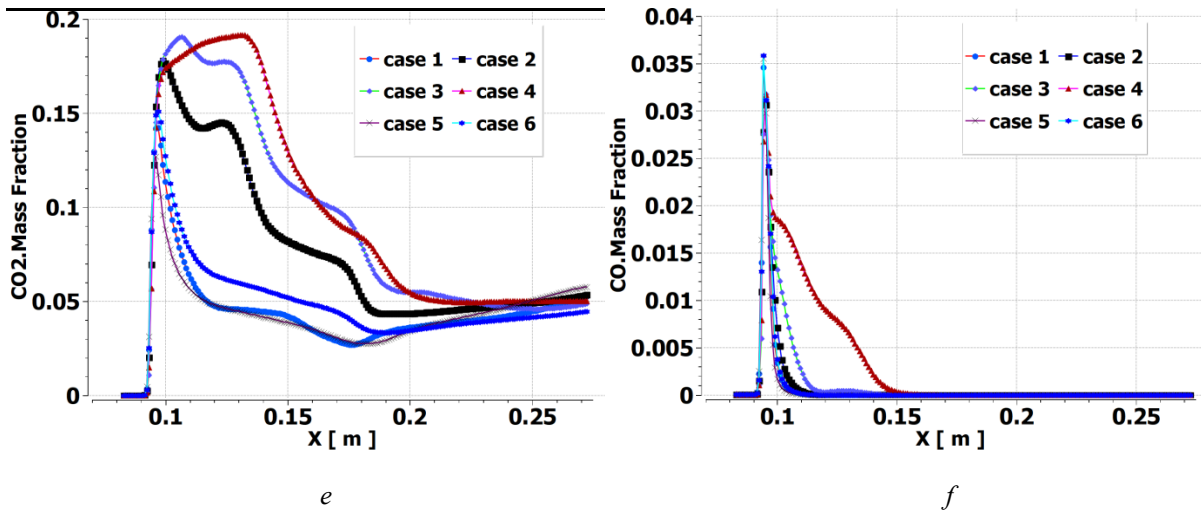


Fig. 11 – Total temperature, velocity fluctuations, O₂, NO, CO₂, CO mass fraction distribution along the combustor liner for: *a* – case 1; *b* – case 2; *c* – case 3; *d* – case 4; *e* – case 5; *f* – case 6

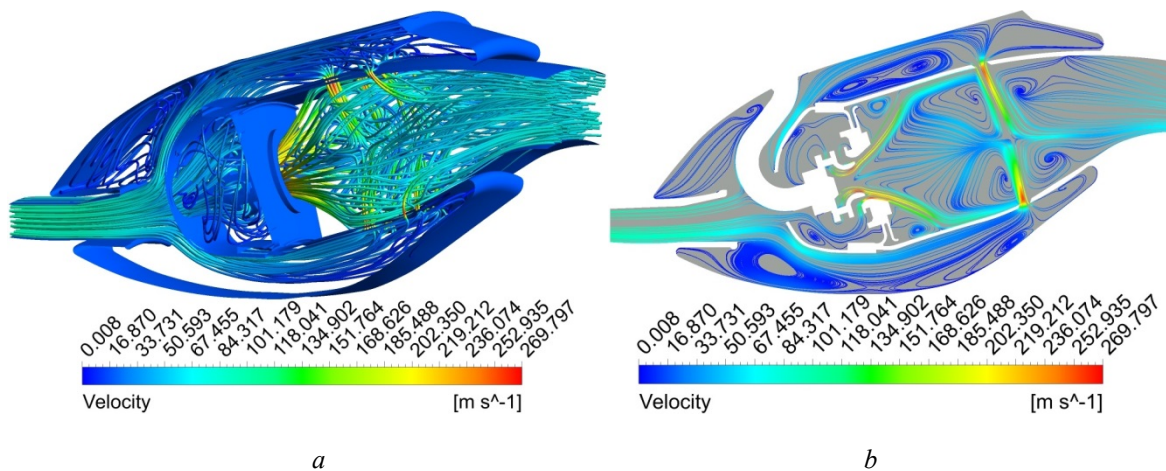


Fig. 12 – The flow passing characteristic: *a* – 3D streamlines; *b* – recirculation zone on cross section plane

Wall temperature of the liners

In Fig 10, as observed from *a* (case 1) to *f* case 6, high temperatures and temperature gradient are predicted on the outer and inner liner walls. The hole location and the number of rows in case 1 shows the maximum temperature of 2077 K. These high temperature region on liner can be seen around the primary zone of the combustion which can be seen around the first row of the liner. The wall temperature decrease around the second rows of holes downstream to the dilution zone region. As we moved the holes to the primary combustion zone in case 2, we can see that the wall temperature around the first row of the holes, decrease and beside that we have the maximum temperature of 2031 K around the second rows of holes in the left side. In this case the flame stretched up to the outlet exit zone and because of this we can see that the temperature on the walls stretched too up to the liner exit zone. For the case 3 by adding one row of holes to the dilution zone the maximum temperature of 2354 K can be observed around the second row on the middle of the liner wall. The distribution wall temperature

contours on case 4 shows that we have a significant uniformity of temperature around the dilution zone of the combustion because of the extra hole rows on the walls but it can be seen that for some regions on wall we have the maximum temperature of 2042 K. When we change the depth angle of the holes for the second row, it can be seen that the air flow passes from these hole under the specific angle, to the liner and has the maximum temperature of 2111 K and a smooth temperature uniformity can be seen on the walls. Beside that the maximum temperature of 2173 K can be seen for the case 6 by the changing the diameter of the holes 1.25 times more than the holes on liner for the first case.

The graph of CO, NO, CO₂, O₂ concentration, velocity, total temperature along the combustor liner relative to the injector axis

All these graphs are shown in Fig. 11. These graphs show the component characteristic, velocity fluctuation and changing total temperature along the axial distance liner relative to fuel injector axis. It is

clear the flow pattern changes along the liner of combustor with different geometrical parameters of the air admission holes such as their rows number and location on the liner. For the graph of O₂ it is clear that the minimum mass fraction of O₂ has been observed in the high temperature region of the combustor. CO₂ forms in a high temperature region similar the formation of NO as we can see their changing along the combustor liner shown in fig. 10. For the temperature fluctuation it can be seen from the graph, that the maximum temperature fluctuation is for case 4 with maximum numbers of air admission holes on the liner, beside that the minimum temperature fluctuations is for the case 5. The distribution of CO concentration can be seen for all cases and it is clear that we have the maximum fluctuation of CO for the case 4 and the minimum changing if for case 5. For the case 2, 3, 4 it can be seen that the maximum fluctuations of NO formation along the liner which is clear from the graphs.

The 3D stream line, recirculation zone, in the combustor liner

In Fig. 12, the flow stream line and recirculation

zone and the flow vectors in the combustor liner is shown for the case 5 of this investigation. The stream lines are shown at the combustor inlet to outlet, the flow fluctuations can be seen in the flow swirling regions in all zone of the combustor liner and the air flow passing through the air admission holes in to the liner are is presented. Including the recirculation zone these models are selected to show strategy of the flow characteristics in 3D form of CFD simulation of the combustion phenomena.

A shortcut for results including the pattern factor and pressure loss

The pattern factor or the uniformity of the temperature at the outlet and the pressure loss is one of the important parameters for designing the aero-engine combustor which has been described in [2] all the results of this simulation are presented in table 1 such as the maximum and the average and the minimum temperature and NO concentration at the outlet of combustor liner including the maximum and the minimum and the average wall temperature.

Table 1 – shortcut to the simulation result

case	1	2	3	4	5	6
Tmin@outlet (K)	1345.94	1346.62	1353.55	1285.75	1363.02	1296.96
Tmax@outlet(K)	1646.06	1692.23	1688.5	1552.61	1586.21	1667.52
Tavr@outlet (K)	1435.59	1435.89	1434.62	1435.14	1434.72	1433.67
NOmin@outlet (ppm)	10.3877	53.8538	276.361	264.92	5.25615	19.0275
NOmax@outlet (ppm)	27.1242	210.337	1260.97	1251.67	10.9412	61.4824
NOavr@outlet (ppm)	14.3577	96.4463	626.264	745.983	6.94215	27.5292
Twallmin (K)	865.012	865.325	865.565	865.804	864.293	865.052
Twallmax (K)	2080.06	2035.03	2354.56	2040.92	2018.27	2177.3
Twallavr(K)	1813.78	1540.83	1667.51	1604.26	1759.99	1829.75
Pressure drop	0.117335	0.116671	0.0782478	0.0595239	0.132063	0.111324
Pattern factor	0.368607	0.448701	0.445731	0.206131	0.26564	0.410981

Conclusion

In this study, the effects of various cases of the geometry and the row number of the air admission holes, on the liner flow balance between the outer and inner liners of the aircraft gas turbine engine combustor, on NO_x and temperature distribution at the outlet exit plane of the liner were predicted using computational fluid dynamics (CFD). The results indicated that the use of CFD allows qualitative prediction of the flow inside the combustor and NO_x performance including the flow pattern and temperature distribution.

An integrated approach to the modification of the aero-engine combustors has been applied for the minimum level. The combustor is annular type, with a liquid fuel atomizer or spray. A final configuration was found and refined by means of a slightly more detailed modelization, comprehensive of the cooling flows simulation with the design of air admission holes on the liner. Then the evaluation of the predicted

performance of the optimal combustor with a fully 3D numerical model has been carried out, which could take into account the discrete nature of the secondary and dilution hole rows. The result was a combustor configuration characterized by promising values of both Pattern Factor, about 0.206 and 0.26 for the cases 4, 5, and emissions, with expected values of average NO concentrations less than 15 ppm for the respectively at 23 % O₂. Beside this the combustor pressure drop changed directly with changing the number and the rows air admission holes. Significant topics of the research was the demonstration of the usefulness of advanced optimization techniques in combustor design and the preliminary validation of the combustion-emission model, a 2-step implementation of the EDM/FRC one, completed with the thermal and prompt NO_x formation mechanism.

References (transliterated)

1. Fuligno, L., Micheli, D., and Poloni, C. (2009), "An Integrated Approach for Optimal Design of Micro Gas Turbine Combustors", *J. Therm. Sci.*, No. 18(2), pp. 173–184.
2. Lefebvre, A. H. (1998), *Gas Turbine Combustion, Second Edition*, Taylor & Francis, New York, USA.
3. Colannino, J. (2015), *Reducing NOx Emissions From Combustion Systems*, Available at: <https://www.chem.info/blog/2015/07/reducing-nox-emissions-combustion-systems> (accessed 30.01.2018).
4. WORLD BANK GROUP (1998), *Nitrogen Oxides: Pollution Prevention and Control Effective*, July, pp. 245–249.
5. Kurose, R., Akamatsu F. (2008), "Experiments and Numerical Simulations of Spray Combustion", *Journal of Combustion Society of Japan*, Vol. 50, pp. 206–214.
6. Moriai, H. D. (2014), "Effects of Dilution Flow Balance and Double-wall Liner on NOx Emission in Aircraft Gas Turbine Engine Combustors", *Mitsubishi Heavy Industries Technical Review*, Vol. 51, No. 4, pp. 9–15.
7. Koutsenko, I. G., Oegin, S. F. and Sipatov, A. M. (2004), "Application of CFD Based Analysis Technique for Design and Optimization of Gas Turbine Combustors", *ASME Paper*, No. GT 2004-53398.
8. Rudolph Dudebout, Bob Reynolds and Khosro Molla-Hosseini (2004), "Integrated Process for CFD Modeling and Optimization of Gas Turbine Combustors", *ASME Paper*, No. GT 2004-54011.
9. Constantinescu, G., Mahesh, K., Apte, S., Iaccarino, G., Ham, F. and Moin, P. (2003), "A New Paradigm for Simulation of Turbulent Combustion in Realistic Gas Turbine Combustors Using LES", *Proceedings of ASME Turbo Expo 2003*, GT 2003-38356.
10. Leiyong Jiang and Ian Campbell. (2010), "An Attempt at Large Eddy Simulation for Combustor Modeling", *Proceedings of ASME Turbo Expo 2010*, GT 2010-22257.
11. James, S., Anand, M. S. and Sekar, B. (2008), "Towards Improved Prediction of Aero-Engine Combustor Performance Using Large Eddy Simulations", *Proceedings of ASME Turbo Expo 2008*, GT 2008-50199.
12. ANSYS, Inc. (2015), *ANSYS CFX-Solver Theory Guide*, United states.
13. Magnussen B. F. and Hjertager B. H. (1977), "On mathematical modeling of turbulent combustion with special emphasis on soot formation and combustion", *Proc. Combust. Inst.*, No. 16(1), pp. 719–729.
14. Valachovic T. G. (1993), "Numerical predictions of idle power emissions from gas turbine combustors", *ASME 1993 International Gas Turbine and Aeroengine Congress and Exposition, American Society of Mechanical Engineers*, 93-GT-175.

Received 03.02.2018

Відомості про авторів / Сведения об авторах / About the Authors

Долматов Дмитро Анатольович (Долматов Дмитрий Анатольевич, Dolmatov Dmytro Anatolyevich) – доктор технічних наук, провідний науковий співробітник кафедри конструкції авіаційних двигунів Національного аерокосмічного університету ім. М. Е. Жуковського «ХАІ», м. Харків, Україна; e-mail: ditrihantelson@yahoo.com.

Хаджіванд Масуд (Хадживанд Масуд, Hajivand Masoud) – аспірант кафедри конструкції авіаційних двигунів Національного аерокосмічного університету ім. М. Е. Жуковського «ХАІ», м. Харків, Україна; e-mail: m.hajivand82@gmail.com.